

Finite Element Analyses for Centrifuge Modelling of Narrow MSE Walls

K-H Yang, Dept. of Civil Architectural and Environmental Engineering, Univ. of Texas at Austin, TX, USA

K.T. Kniss, Hayward Baker Inc, USA

J.G.Zornberg, Dept. of Civil Architectural and Environmental Engineering, Univ. of Texas at Austin, TX, USA

S.G. Wright, Dept. of Civil Architectural and Environmental Engineering, Univ. of Texas at Austin, TX, USA

ABSTRACT

High transportation demand has led to widening of existing roadways to improve traffic flow. In some cases, the space available on site is limited and the construction of earth retaining walls is done in front of previously stabilized walls. This can lead to retaining wall designs that are narrower than those addressed in current design guidelines. Narrow walls are Mechanically Stabilized Earth (MSE) walls having an aspect ratio (L/H) less than 0.70. Previous studies have suggested that the internal and external behavior of narrow retaining walls differ from that of traditional walls. This paper presents a study of the behavior of narrow MSE wall models tested in a centrifuge using the finite element program Plaxis. The results predicted by the finite element model are in a good agreement with the experimental data from centrifuge tests at working stress and failure conditions. Finite element study also shows that a zero pressure zone is observed at the interface between the reinforced backfill and stable wall and extends farther below the surface as the wall width becomes narrower. As a result of this zero pressure zone, the crest of the MSE wall has a tendency to settle at the interface. This settlement leads to instability and, finally, the failure of the wall. The implications of the finite element study are addressed in this paper as design considerations to improve the stability of narrow walls.

1. INTRODUCTION

As the population increases and development of urban areas becomes a priority, transportation demand has increased which has led to widening of existing highways to improve traffic flow. One solution is to build mechanically stabilized earth (MSE) walls in front of previously stabilized walls. However, due to the high cost of additional right-of-way and limited space available at job sites, construction of earth retaining walls is often done under a constrained space. This leads to retaining walls that are narrower than in current design guidelines. Narrow walls, herein, are referred as Mechanically Stabilized Earth (MSE) walls having an aspect ratio (L/H) less than 0.70.

Various studies suggest the internal and external behavior of narrow retaining walls is different from that of traditional walls. For example, Frydman and Keissar (1987) and Take and Valsangkar (2001) performed centrifuge tests, Leshchinsky and Hu (2003) and Lawson and Yee (2005) conducted limit equilibrium analyses, Kniss et al. (2007) used finite element analyses to study the earth pressures of narrow walls. They all concluded that, due to arching effect, the earth pressure coefficient decreased as wall aspect ratio, ratio of wall width to wall height (L/H), decreased. This implies that the traditional method using conventional earth pressure equations to calculate the factor of safety against breakage is not appropriate for narrow walls.

Woodruff (2003) performed a comprehensive series of centrifuge model tests on reinforced soil walls adjacent to a stable face. Two important observations were drawn from his tests. First, the failure planes are bilinear and have an inclination less than the theoretical Rankine linear failure plane. This suggests the traditional method which assumes the Rankine failure plane to evaluate the factor of safety against pullout is not applicable for narrow walls. Second, Woodruff observed that when the wall aspect ratio decreased below 0.25, the failure mode changed from internal failure to external failure. He reported the external failure initiated from a "trench" at the interface between the reinforced backfill and stable wall and this trench had a tendency to pull MSE wall away from the stable wall resulting in external failure. This implicates that, besides the issues of internal stability, the external stability for narrow walls may be required a different consideration from that for conventional walls. A summary of dominant failure modes and corresponding design methods for various aspect ratios is provided in Table 1.

Table 1. Summary of wall failure modes and design methods

Wall Aspect Ratio	$L/H < 0.3$	$0.3 < L/H < 0.7$	$L/H > 0.7$
Failure Mode	External	Compound	Internal
Design Method	Cement Stabilized Wall*	FHWA SMSE Wall Design Guidelines (Morrison et al. 2006)	FHWA MSE Wall Design Guidelines (Elias et al., 2001)

* Cement stabilized wall is suggested by local engineering company

Although the FHWA design guidelines for shored mechanically stabilized earth (SMSE) wall systems are suggested for the design of MSE walls with aspect ratios from 0.3 to 0.7, several important characteristics of narrow MSE walls are not considered in these guidelines. For example, the guidelines make no allowances for a reduction in earth pressure due to arching effect. Besides, the SMSE wall guidelines also suggests to neglect to check the external stability. With those inconsistencies in mind, the purpose of this study is to better understand the behavior of narrow walls, establish design guidelines especially for narrow MSE walls, and expect to extend the application of narrow MSE walls even at aspect ratio below 0.3.

This paper will review the centrifuge tests reported in Woodruff's thesis (2003) and compare them to finite element simulations corresponding to two centrifuge tests. The first simulation is compared to centrifuge test in detail at both working stress and failure conditions. This comparison would be treated as a verification of finite element model. The first simulation is also used to study the mechanics of "trench", observed from centrifuge test as a premonitory symptom of failure. Then, second simulation is used as a parametric study to understand how this trench grows as the decrease of wall aspect ratio. Finally, implications learned from finite element study are addressed as design considerations to improve the stability of narrow walls.

2. CENTRIFUGE MODEL

A series of centrifuge model tests on reinforced soil walls adjacent to a stable face was performed by Woodruff (2003) under the supervision of Dr. Zornberg at the University of Colorado at Boulder. He tested 24 different walls with reinforcement lengths (wall widths) ranging from 0.17 to 0.9 times the wall height. All the reduced-scale walls were 230 mm tall and the wall facing batter was 11 vertical to 1 horizontal. Monterey No. 30 sand was used as the backfill material. The target backfill relative density of 70% was reached by pluviating the sand from a height of 120 mm. The reinforcements used in centrifuge study were the commercially available nonwoven geotextile and had two types: Pellon True-grid and Pellon Sew-in. Pellon True-grid was a white 60% polyester and 40% rayon fabric with mass per unit area of 28 g/m². The fabric, tested by wide width strip tensile tests (ASTM D4595), had strength of 0.09 kN/m in machine direction and 1 kN/m in the transverse direction and referred as R2 and R4, respectively. Pellon Sew-in was a white 100% polyester fabric with a unit weight of 24.5 g/m². The fabric had strength of 0.03 kN/m in machine direction and 0.1 kN/m in the transverse direction and referred as R1 and R3, respectively.

Tests were performed with reinforcement of different tensile strengths, and reinforcement layouts involving five different vertical spacings. Woodruff loaded each wall to failure and recorded the load (acceleration "g" force) required to fail the wall. The pictures, in Figure 1, shows a series of responses observed from one of these tests (Test 2b, L/H=0.4), which was subjected to increased gravitational forces in a geotechnical centrifuge until failure occurred. Figure 1c shows the settlement is occurred at back side of crest, which initiates the collapse of the wall. Horizontal lines (colored sand) shown in the pictures indicate the location of geosynthetic reinforcements.

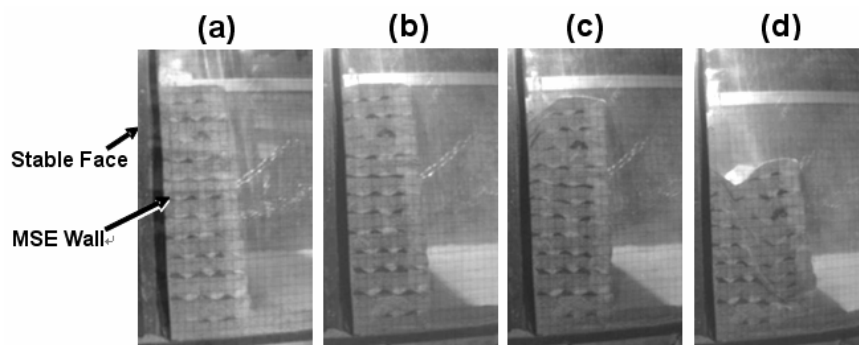


Figure 1. Photographic images from centrifuge: (a) Initial condition (gravity); (b) Working Stresses (10g); (c) Before Failure (41g); (d) Failure condition (41g) (from Woodruff, 2003)

High-speed video cameras were used to record the deformations of the wall. The location of the failure surface was determined based on observed tears (rupture) in each layer of reinforcement. The tests revealed failure surfaces ranging from one entirely through the reinforced soil zone, to compound surfaces that formed partially through the reinforced soil and partially along the interface between the reinforced soil and stable face. Figure 2 shows an example of compound failure from Test 2b. The upper four layers of reinforcements pulled away from the stable face and breakage occurred at the lower layers of reinforcements.

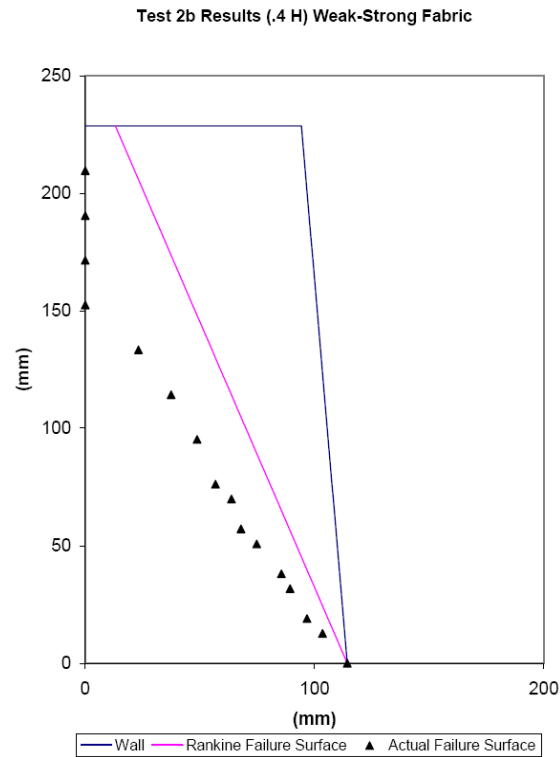


Figure 2. An example of compound failure at Test 2b (from Woodruff, 2003)

3. NUMERICAL MODEL

The finite element program Plaxis version 8.2 (Plaxis, 2005) was used to conduct the numerical analysis reported herein. Finite element simulations were performed to model centrifuge tests 2b and 5c. A summary of the condition and result of these two centrifuge tests is listed in Table 2

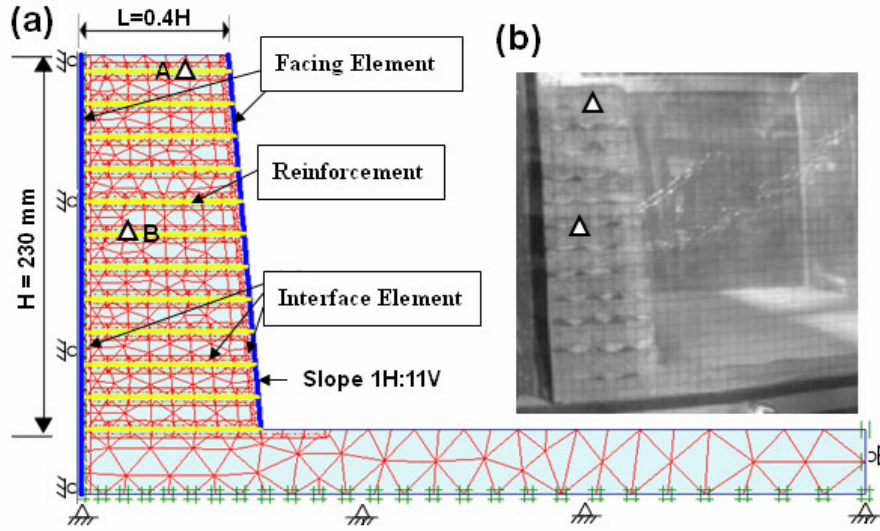
Table 2. Summary of centrifuge tests 2b and 5c (from Woodruff, 2003)

Test	G@Failure	Reinforcement Length	Reinforcement Strength	Stable Face	Wall Face	Failure Type	G@Pull away	Spacing (mm)
2b	41	0.4H	R2	Aluminum	Wrap Around	Compound	39	20
5c	32	0.25H	R4	Aluminum	Wrap Around	External	13	20

3.1 Initial Geometry and Boundary Condition

Figure 3a shows the numerical model of centrifuge test 2b. The finite element meshes are composed of 15-node isoparametric triangular elements. The mesh coarseness was set as “Fine”, which would generate around 500 triangular elements for a given geometry. Horizontal fixities (rollers) were applied to the stable face. This allowed the wall to settle at in the vertical direction but prohibited the nodes along the boundary from moving laterally. Total fixities were placed at bottom of the foundation. Plane strain was assumed to solve the three-dimensional problem with a two-dimensional analysis.

Stage construction was included by conducting layer-by layer construction in Plaxis. The centrifugal force of the centrifuge was simulated by increasing the body force on the wall model. This technique allows the simulation to follow a more realistic loading path and to produce more representative results than the conventional modeling technique. In conventional modeling technique, the effect of centrifugal force was modeling by rescaling the reduced wall into prototype. Updated mesh analysis was activated to take into account for the effect of large deformation, especially important at failure condition.



Note: Triangle A and B are the locations of sand markers used to tracking the displacement in reinforcement at working stress condition

Figure 3. Wall geometry of Test 2b: (a) Finite element setup and initial mesh; (b) Picture from centrifuge at initial condition

3.2 Backfill Model and Material Properties

The backfill soil material used in the centrifuge was Monterey No. 30 sand. Hardening Soil model was selected to simulate the nonlinearly plastic response. The Hardening Soil model is a stress-dependent hyperbolic model based on the flow rule and plasticity theory. It was believed that Hardening Soil model had better ability to match the stress-strain curves of granular soil at working stress conditions than the Mohr-Coulomb model, a linear elastic and perfect plastic model. Angle of dilatancy (ψ) was used to account for the dilatation of sand during shearing. The value was calculated by the empirical equation $\psi \approx \phi - 30^\circ$ (Bolton, 1986). Another important matter was the sensitivity of the soil properties to relative compaction density. Therefore, three triaxial compression tests by Li (2002) with specimen relative density 65% (close to 70%) were used to calibrate the backfill parameters. Figure 4 shows the result of calibration. The parameters of the Hardening Soil model are listed in Table 3.

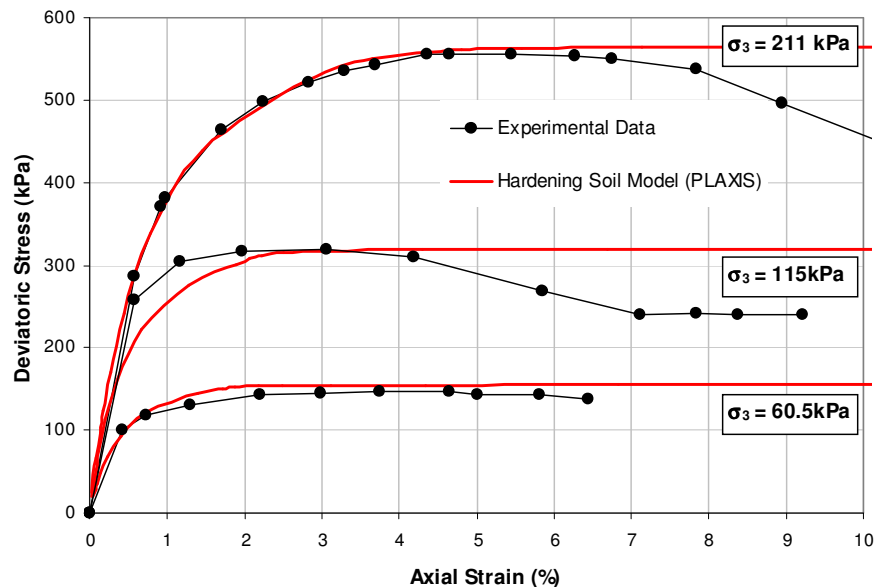


Figure 4. Stress-strain curves for drained triaxial tests on Monterey #30 sand

Table 3. Material properties for sand backfill

Bulk unit weight of backfill	Value
γ (unit weight) (kN/m ³)	16.05
Strenght properties	
ϕ (peak friction angle) (degrees)	36.7
c (cohesion) (kPa)	5 ⁽¹⁾
ψ (angle of dilatancy) (degrees)	6.7
Stiffness properties (Hardening Soil model)	
E_{50}^{ref} (secant stiffness) (kPa)	35000
E_{ur}^{ref} (unloading/reloading stiffness) (kPa)	105000 ⁽²⁾
E_{ode}^{ref} (tangent stiffness for primary odeometer loading) (kPa)	60000
m (modulus exponent)	0.5
R_f (failure ratio)	0.85
u_{ur} (Poisson's ratio for unloading/reloading)	0.2

Note: (1) Cohesion was set a small value for numerical purpose

(2) E_{ur}^{ref} was assumed to be $3E_{50}^{ref}$ as the default value in Plaxis

3.3 Reinforcement and Facing Models and Material Properties

The reinforcements were modeled as line elements with a normal stiffness but with no bending stiffness. In addition, line elements could only sustain tensile forces but no compression. An elastoplastic model was selected to mimic the breakage of reinforcement. The input parameters for the reinforcements were the elastic axial stiffness EA and maximum axial tension force, N_p . The value of EA was determined as the secant modulus at 2% strain from the wide width tensile test. The value of N_p was adopted from the peak strength of the wide width tensile test. An average back-calculated strength ratio (≈ 2.5) reported by Woodruff was used to account for the difference between unconfined and confined conditions. A summary of reinforcement parameters are listed in Table 4.

Table 4. Material properties for reinforcement and facing elements

Reinforcement	Value
R2 (weak direction)	
EA (axial stiffness) (kN/m)	1.25
N_p (maximum tensile strength) (kN/m)	0.0225
R4 (strong direction)	
EA (axial stiffness) (kN/m)	1.4
N_p (maximum tensile strength) (kN/m)	0.025
Facing elements	
Wall face (geotextile-wrap around)	
EI (bending stiffness) (kNm ² /m)	1.2
EA(bending stiffness) (kN/m)	502
Stable face (Aluminum)	
EI (bending stiffness) (kNm ² /m)	10000
EA(bending stiffness) (kN/m)	10000

Plate elements were used to represent the wall face. Plates are structural objects composed of beam elements with bending stiffness, EI, and normal stiffness, EA. The values of EI and EA for the stable face were set high enough to prohibit the deformation occurring in the stable face. A parametric study was performed to find the appropriate input values for simulating a flexible wall, e.g. geotextile wrap around face. The finally EI and EA values were selected by the criteria that the earth pressure along the wall face was no longer decreased with the decrease of EI and EA values. A summary of facing parameters are listed in Table 4.

3.4 Interface Models and Material Properties

A previous study by Kniss et al. (2007) successfully captured the reduction of earth pressure due to the arching effect by employing interface elements. In this study, interface elements were introduced adjacent to the wall face, stable face and reinforcement elements to capture the soil-structure interaction. The material properties of an interface element correspond with backfill properties; however, the strength of the interface can be controlled by the interface reduction factor, R_{inter} . The value of R_{inter} depended on the roughness of the surface; 1/3 was assigned to the soil-stable face (aluminum) interface elements and 0.9 to the soil-wall face (geotextile) and soil-reinforcement (geotextile) elements.

4. RESULTS

The analytical results of Test 2b were compared to the results measured from centrifuge test at working stress and failure conditions. These comparisons showed the finite element simulations can capture the behavior of a centrifuge test. The simulation of Test 2b was also used to study the mechanics of the “trench”. The simulation of Test 5c was used as a parametric study to understand how this trench develops with the decrease of wall aspect ratio.

4.1 Working Stress Condition

As mentioned previously, a body force was applied to simulate the centrifugal force. The magnitude of the applied body force is a multiple of the force applied by gravity. For example, the body force 2g would be equivalent to twice the force applied by gravity. Location A and B (see Figure 3) were selected to track the relative displacements between an applied body force equal from 3g to 10g. Because of the centrifuge data not reliable at low g-levels, the displacement data below 3g was not included. The relative displacements were calculated from the following distance equation:

$$d = \sqrt{(x_{Ng} - x_{3g})^2 + (y_{Ng} - y_{3g})^2} \quad \text{eq.(1)}$$

where

d is the relative displacement between 3g and Ng; N is any interested g-level;

x_{3g} and y_{3g} are the coordinate of location A or B at 3g;

x_{Ng} and y_{Ng} are the coordinate of location A or B at Ng.

The coordinates were determined by importing the camera-recorded images into an image processing program. Figure 5 shows the comparisons of results between experimental measurements and measurements from the finite element analysis. The general trends show good agreement at locations A and B. The discrepancies may be the result of the human error of tracking the selected locations or from the low resolution of the images.

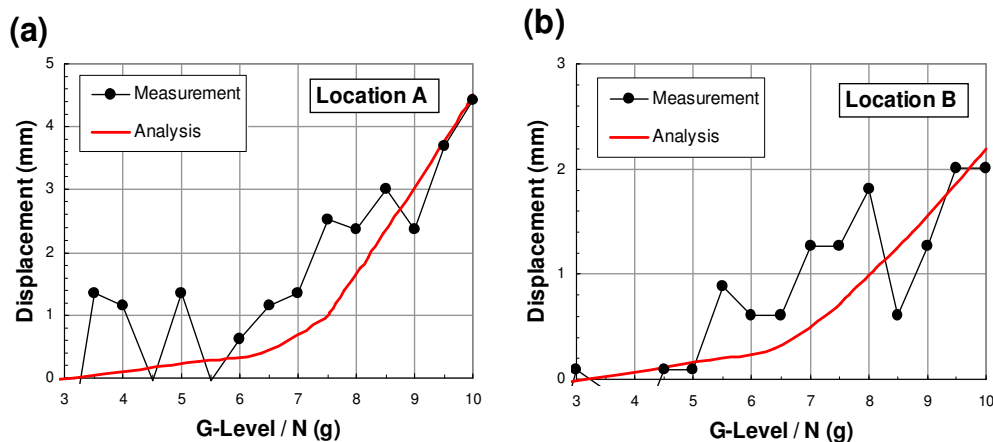


Figure 5. Comparison of displacement at working stress condition: (a) Location A; (b) Location B

4.2 Failure Condition

After applying a body force equal to 10g, a Phi-C reduction function was selected at next calculation phase. In Phi-C reduction function, the strength parameters $\tan\phi$ and c of the soil are successively reduced until failure of the structure occurs. The strength of the interfaces is also reduced in the same way. Another benefit is that the global factor of safety can be obtained by this approach. The factor of safety is defined as ratio of available soil strength to strength at failure. This factor of safety is conventionally used to evaluate the stability of MSE walls. The failure characteristics observed from the finite element simulation and centrifuge test were compared. In Figure 6a and 6b, the displacement contours produced from the finite element simulation shows a similar displacement vector with the image from the centrifuge which was shot at the moment of failure. Both models showed a sliding down of upper layer wall and a stationary triangular part at bottom of wall.

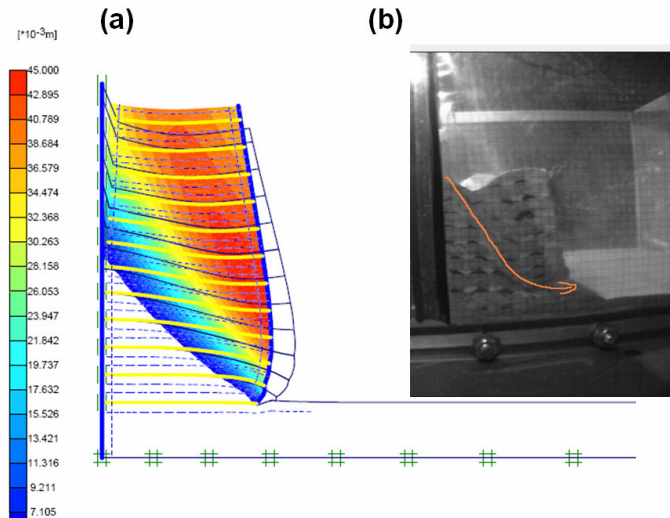


Figure 6. Comparison of displacement: (a) displacement contour from finite element simulation; (b) Image from centrifuge.

As shown in Figure 2 and Table 2, the failure mode of Test 2b was defined as a compound failure. The finite element simulation also reproduced this phenomenon. Figure 7a shows a summary of calculated maximum tensile force at each reinforcement layer and Figure 7b shows the actual reinforcements after the centrifuge test. In Figure 7b, the maximum tensile force reaching ultimate tensile strength (input value) means the breakage of the reinforcement at lower layers (from #1 to #7); the developed tensile force less than ultimate strength means that no breakage of reinforcement occurred at upper layers (from #8 to #12). In Figure 7b, the experimental results showed that the lower eight layer reinforcements broke and the upper four layers did not. The experimental results supported the calculation results.

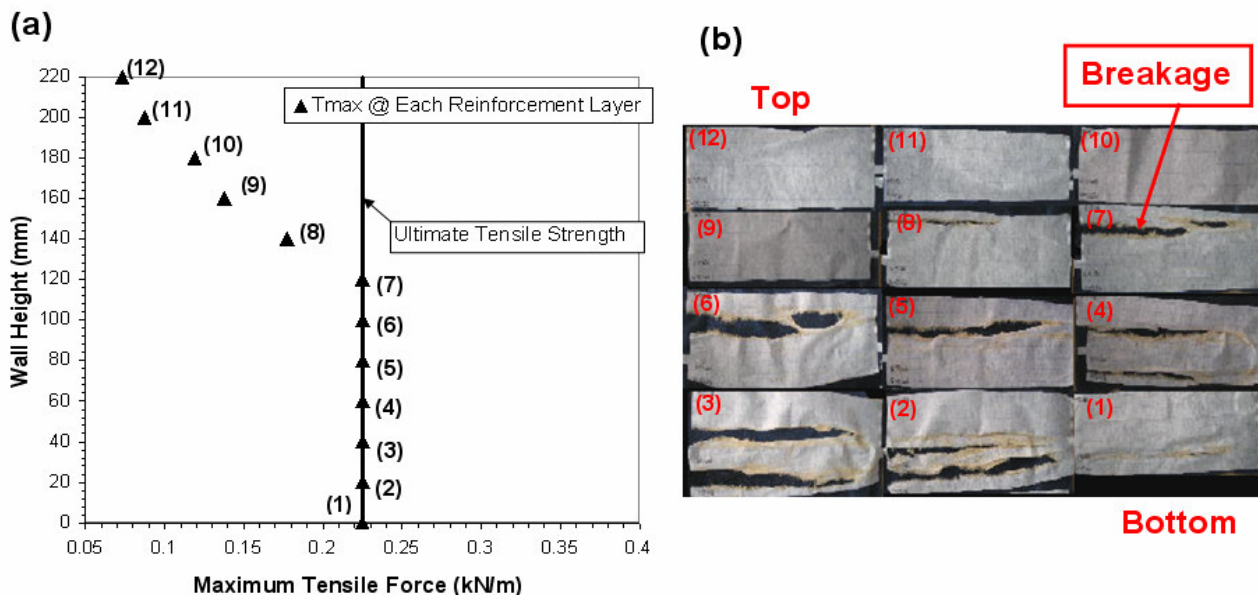


Figure 7. Comparison of breakage of reinforcements: (a) Results from finite element simulation; (b) Image of reinforcement.

4.3 Development of a Zero Pressure Zone

The normal stress acting on the interface between wall and stable face was examined to monitor the formation and mechanics of the trench. The interface element has zero thickness; therefore, the normal stress acting on the interface is identical to act on the stable face. A maximum tensile force equal to 1 kN/m (default is zero) was allowed to make identification of the tensile points more obvious in Figure 8a and 8b. Figure 8a shows the distribution of normal stresses along the interface for Test 2b. Positive normal stress means compression and negative means tension. The results in Figure 8a suggest the trench observed by Woodruff was actually a tension crack. The tension crack was initiated along the interface between the soil and stable face and extended to a depth of approximately 0.43H for the wall with aspect ratio 0.4.

Test 5c was performed as a parametric study to understand how the tension crack develops with the decrease of wall aspect ratio. The procedure of simulating Test 5c coincided with that of Test 2b and won't be repeated herein. Figure 8b shows the distribution of normal stresses along the interface for Test 5c. Comparing Test 2b and Test 5c, the tension crack increased in depth from around 43% to 87% of the wall height as wall aspect ratio decreases from 0.4 to 0.25. It may be fare to say the length of tension crack could reach entire wall height at wall aspect ratio 0.25, regardless of few spikes of normal stress around the bottom part of wall.

The tension may be the by-product from assuming a small cohesion for the soil constitutive model which must be done to avoid numerical instabilities. Besides, there may be a doubt about the true existence of tension of sand or gravel material to pull MSE wall away from stable face to cause failure. However, in the authors' opinion, the most important fact is that there was no normal stress or zero pressure zone developing along the stable face. This could cause the backfill material to leak and settle along the crack, as observed from centrifuge test (see Figure 1c), and then lead to redistribution of stress and ultimately the instability and failure of the wall.

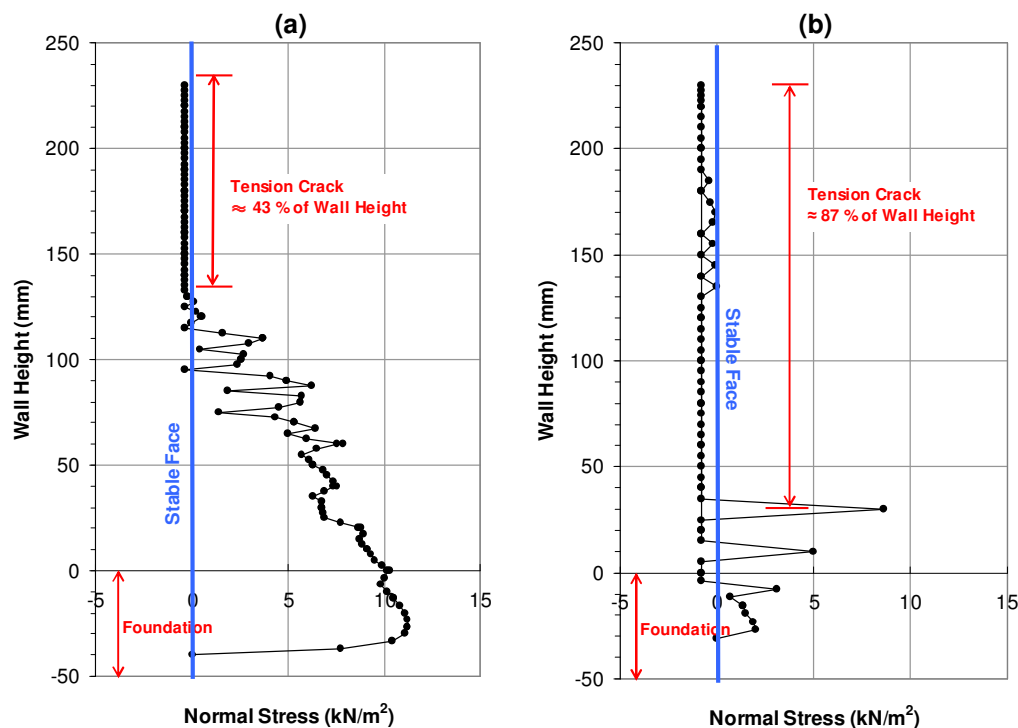


Figure 8. Distribution of normal stress along interface face: (a) Test 2b; (b) Test 5c.

5. IMPLICAITONS FROM FINITE ELEMENT SIMULATION

Without the accurate pressure cell measurements, the centrifuge modeling only can reveal information about the displacement and deformation of the wall. The stress distribution is important to understanding the failure mechanism and the mechanics behind it. Fortunately, this information can be unveiled from a well calibrated finite element simulation. Figure 9 shows stress points from the finite element simulation of Test 2b at failure. The plastic point in Figure 9 means the stress of soil at that point is beyond the elastic region into the plastic region. Plastic point can be conceived as the

failure of soil at that point. The tension point in Figure 9 indicates the stress state is under the tension instead of compression. Based on Figure 9, four design considerations to prevent the wall from falling are listed. Each design consideration corresponds to the numbers indicated in the Figure 9.

1. Eliminate tension points at interface:

the possible solutions are that attaching reinforcements to stable face or extending upper reinforcements over existing wall.

2. Limit large deformation of front face:

the possible solution is that using rigid face (e.g. concrete panel or block) rather than flexible face (e.g. geosynthetics wrap around).

3. Diminish plastic points in the wall:

the possible solutions involve increasing strength of backfill, i.e. high strength backfill or high compaction effort, or increasing the strength function of reinforcement.

4. Attenuate plastic points in the foundation:

Figure 9 shows the plastic points would spread to foundation. The methods of improving the strength of foundation could be considered.

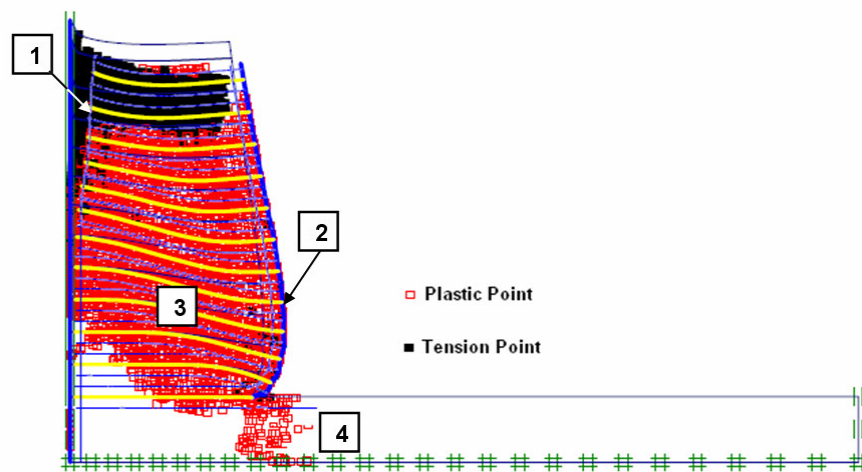


Figure 9. Stress points of Test 2b at failure condition

6. CONCLUSIONS

This paper presented a finite element simulation to better understand the behavior and mechanics of narrow MSE walls. The results predicted by the finite element model were compared to the results from centrifuge test at working stress and failure conditions. The results matched well. The stress information from the finite element simulation helped to understand the formation and mechanics of the trench observed at the interface between MSE and stable walls. Interpretation of the stress information showed that the failure of narrow MSE wall was initially caused by a zero pressure zone. This zero pressure zone extends further below the crest as the wall width became narrower and approximately reached the bottom of wall at wall aspect ratio 0.25. As a result of this zero pressure zone, the MSE wall had a tendency to sink into the trench and ultimately cause the failure of the wall. Four design considerations inspired by the finite element simulation were proposed to improve the stability of the wall. The successful simulation of this study could serve as an exemplar of designing narrow MSE walls by using the tool of finite element method. For future study, the proposed design considerations could be evaluated by the finite element method.

ACKNOWLEDGEMENTS

The presented work was supported by TxDOT (Project No. 0-5506). The First author is indebted to his undergraduate student, Nichol Cruz, for helping the finite element simulation. Comments from reviewers and editors to improve the paper are appreciated.

REFERENCES

- Bolton, M.D., (1986). "The Strength and Dilatancy of Sands," *Geotechnique*, Vol. 36, No. 1, pp. 65-78.
- Elias, V., Christopher, B.R., and Berg, R.R., (2001), "Mechanically Stabilized Earth Walls and Reinforced Soil Slopes Design and Construction Guidelines," *Report No. FHWA-NHI-00-043*, National Highway Institute, Federal Highway Administration, Washington, D.C. March.
- Frydman, S. and Keissar, I., (1987), "Earth pressure on retaining walls near rock faces," *Journal of Geotechnical Engineering*, ASCE, Vol. 113, No. 6, June, pp. 586-599.
- Kniss, K. T., Yang, K-H, Wright, S. G. and Zornberg, J. G. (2007), "Earth Pressures and Design Consideration of Narrow MSE Walls", *Proceedings of the Conference of Texas Section-ASCE Meeting*, Taylor, Texas, April, 2007
- Lawson, C.R., and Yee, T.W., (2005), "Reinforced soil retaining walls with constrained reinforced fill zones," *Proceedings, Geo-Frontiers 2005*, ASCE Geo-Institute Conference, pp. 2721-2734.
- Leshchinsky, D., Hu, Y. and Han, J., (2004), " Limited reinforced space in segmental retaining walls," *Geotextiles and Geomembranes*, Vol. 22, No. 6, pp. 543-553.
- Li, C., (2002), "Experimental studies on fiber-reinforced soil", *University of Colorado Research Report*.
- Morrison, K.F., Harrison, F.E., Collin, J.G., Dodds, A., Arndt, B. (2006), "Shored Mechanically Stabilized Earth (SMSE) Wall Systems Design Guidelines," *Report No.FHWA-CFL/TD-06-001*, Federal Highway Administration, Central Federal Lands Highway Division.
- PLAXIS (2005). *Plaxis Finite Element Code for Soil and Rock Analyses*, Version 8.2, P.O. Box 572, 2600 AN Delft, The Netherlands (Distributed in the United States by GeoComp Corporation, Boxborough, MA).
- Take, W.A. and Valsangkar (2001), "Earth pressures on unyielding retaining walls of narrow backfill width," *Can. Geotech. Journal*, Vol.38, pp.1220-1230.
- Woodruff, R. (2003), "Centrifuge modeling of MSE-shoring composite walls," Master Thesis, Department of Civil Engineering, the University of Colorado, Boulder.